Supplementary Information

Supplementary Figure 1. Brain AV connection diameter was increased, following homozygous deletion of Rbpj from endothelial cells, but not following heterozygous deletion.

mGFP+ endothelium (green) highlighted AV connection diameters (yellow brackets) in (A) *Rbpj* wild-type, (B) *Rbpj* heterozygous control, and (C) *Rbpj* homozygous mutant. AV connection diameters were significantly increased following homozygous deletion of *Rbpj* compared to *Rbpj* wild-type (females, P = 0.0006; males, P = 0.007) and heterozygous controls (females P = 0.001, males P = 0.0039), while AV diameters remained unchanged between *Rbpj* wild-type and heterozygous controls in (D) female and (E) male mice at P14 (females, P = 0.7524; males, P = 0.8189). (F) Similar results were observed with combined female and male datasets: wild-type vs. homozygous *Rbpj* deletion, P < 0.0001; heterozygous vs. homozygous *Rbpj* deletion, P < 0.0001; wild-type vs. heterozygote control, P = 0.9802. n=3 females and n=3 males for all experimental cohorts.

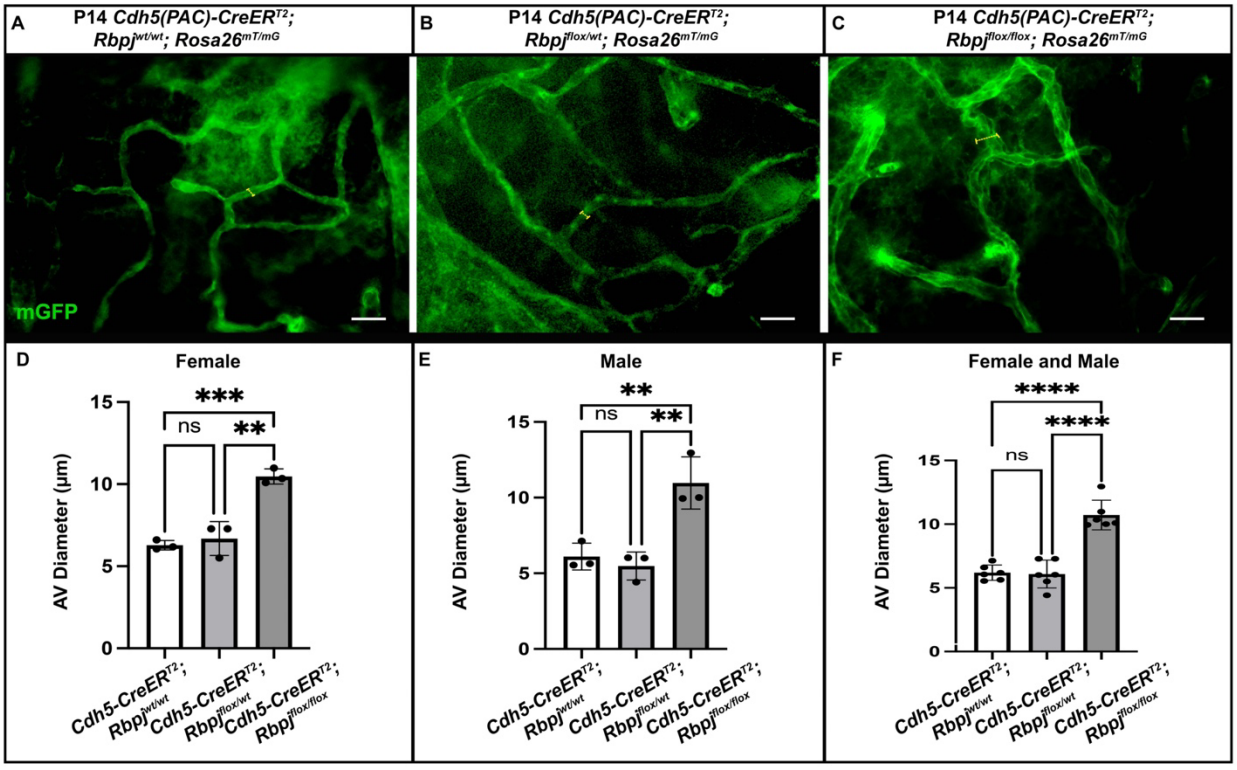

Supplementary Figure 2. A subset of CNS resident macrophages in the early postnatal cerebellum co-expressed Iba1, TMEM119, and CD68.

(A-B) In P14 cerebellum, immunostaining against Iba1 (red) and TMEM119 (green) showed the majority of Iba1+ cells co-express microglia marker TMEM119 in control and mutant tissue. (C-D) High magnification images showed co-localization of Iba1 (red) with microglia markers TMEM119 (green) and CD68 (white). (E) Quantification of the percentage of Iba1+ cells that co-express TMEM119. (F-G) In P21 cerebellum, the majority of Iba1+ cells co-expressed TMEM119 in control and mutant tissue. (H-I) High magnification images showed co-localization of Iba1, TMEM119, and CD68. (J) Quantification of the percentage of Iba1+ cells that co-express TMEM119. n=4 for all cohorts.

Supplementary Figure 2

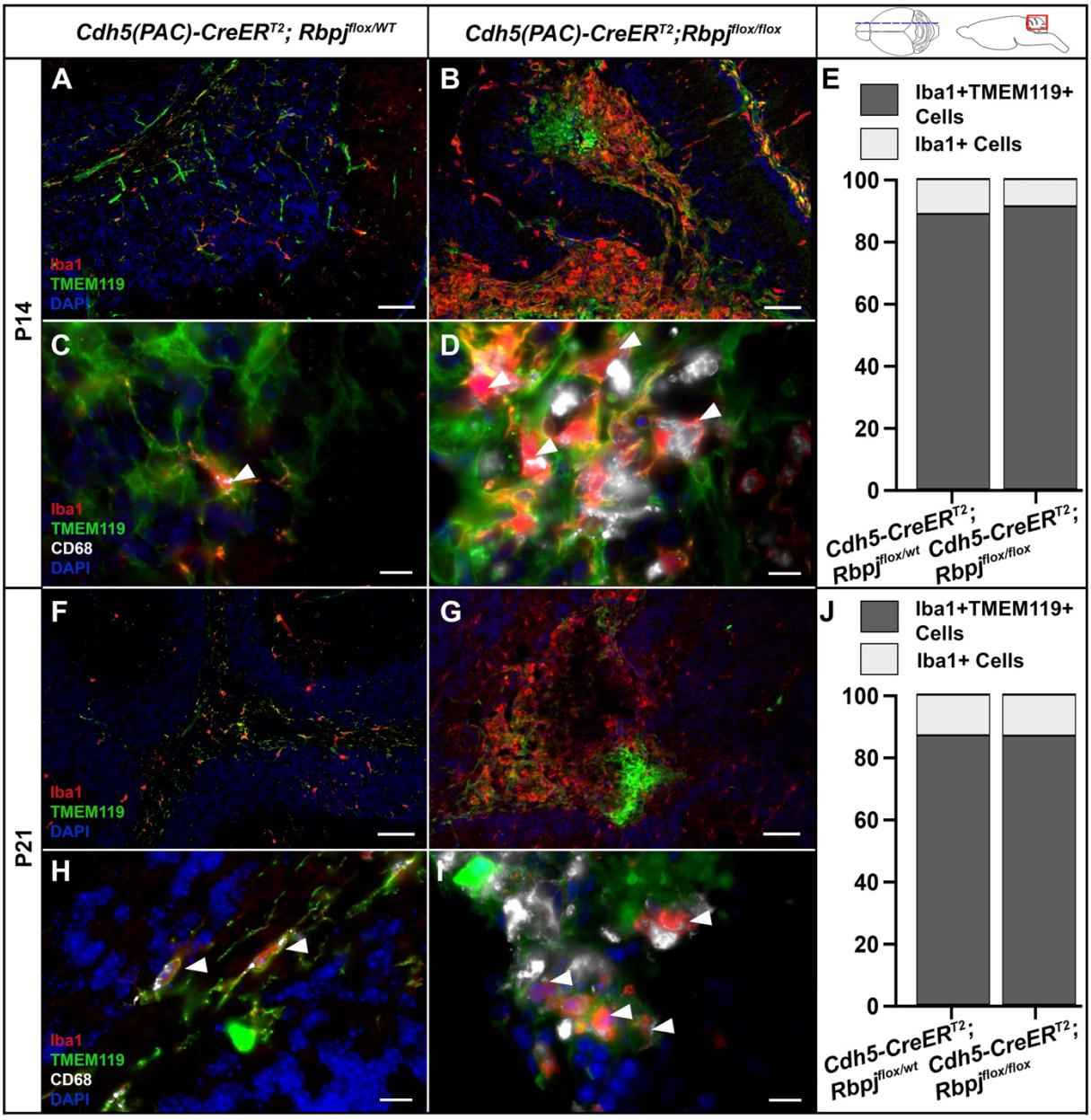

Supplementary Figure 3. Expanded Iba1 expression was observed in mutant cerebellum, as compared to controls, at P14 and P21

(A) Schematic representation of the midsagittal cerebellum regions, for reference. Images highlight CNS resident macrophage distribution and morphology. (B-E') Morphological analysis of CNS resident macrophages immunostained against Iba1 (red) in various regions of the cerebellum. Cerebellum regions were visually demarcated by density of DAPI+ (blue) nuclei. Iba1+;DAPI+ staining of mutant and controls at P14 (B,C) and P21 (D,E) showed expanded Iba1 expression in mutant cerebellum. Iba1 staining without DAPI counterstain for the corresponding P14 (B',C') and P21 (D',E') time points. WM, white matter; GL, granular layer; ML, molecular layer. (F) P21 analysis (two-way ANOVA) showed increased percentage of Iba1+ area, as analyzed by sex. Female control vs. Female mutant, P=0.0244. Male control vs. Male mutant, P=0.0159. Female control vs. Male control, P>0.9999. Female mutant vs. Male mutant, P=0.9846. Females, n=3 controls and n=3 mutants. Males, n=3 controls and n=3 mutants. (F') Percentage of Iba1+ area was increased in a combined dataset, analyzed by Student's *t*-test with Welch's correction, P<0.0001. n=6 control and n=6 mutants. (G) P21 analysis (two-way ANOVA) showed increased number of Iba1+ cells, as analyzed by sex. Female control vs. Female mutant, P=0.0043. Male control vs. Male mutant, P=0.0020. Female control vs. Male control, P>0.9999. Female mutant vs. Male mutant, P=0.8893. (G') Number of Iba1+ cells was increased in a combined dataset, analyzed by Student's *t*-test with Welch's correction, P=0.0004. n=6 control and n=6 mutants.

Supplementary Figure 3

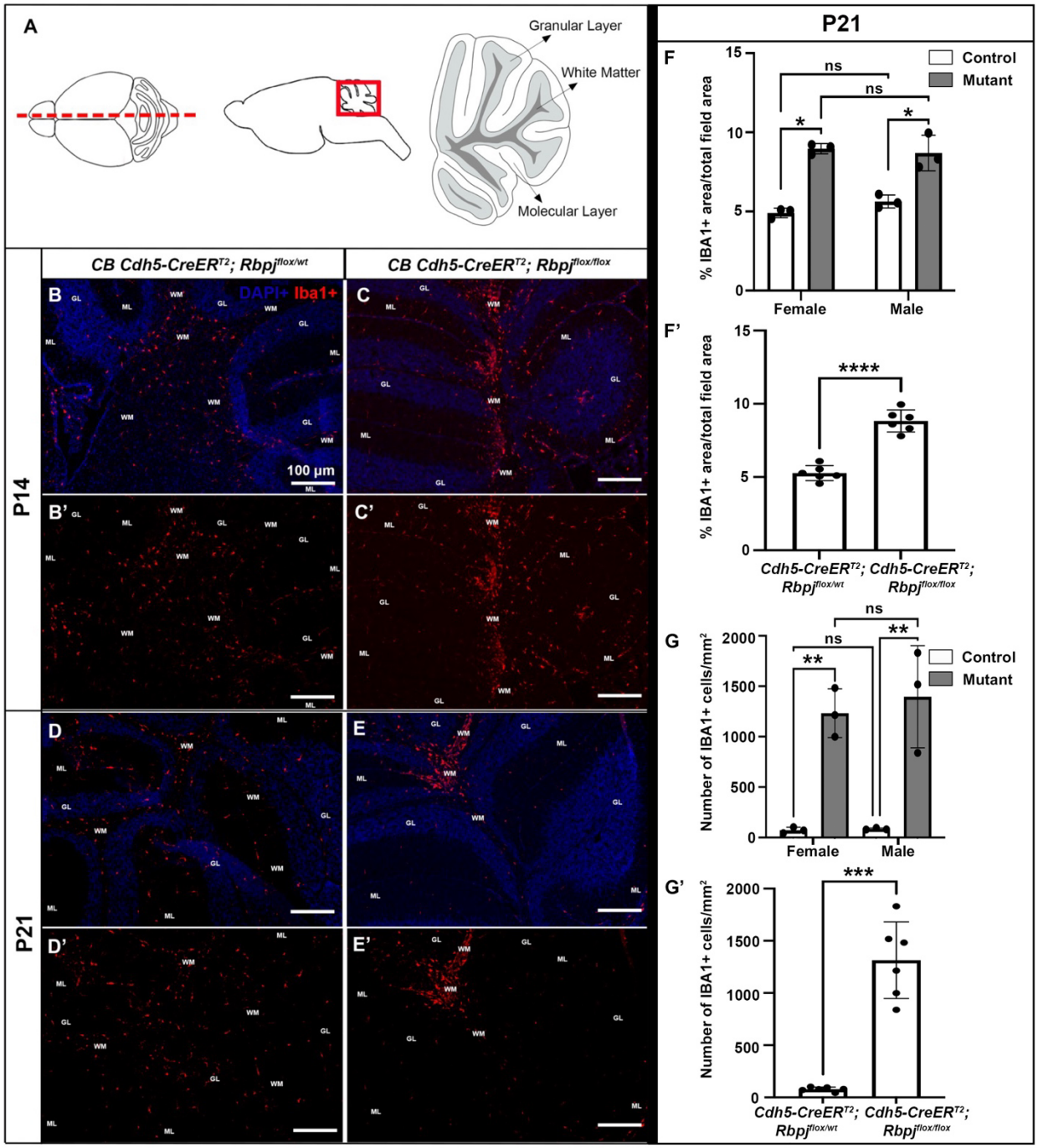

Supplementary Figure 4. CNS resident macrophages exhibited region specific states for Iba1 expression, cell number, and proliferation at P14 and P21 in mutants, as compared to controls

Representative images of (A-A'') control P14 and (B-B'') mutant P14 are shown. Staining is represented with DAPI in blue for cell nuclei, Iba1+ cells in red, and Edu+ proliferative cells in white. Iba1+;Edu+ cells, indicative of proliferative CNS resident macrophages, are circled in white. Three cerebellum regions were analyzed at P14 and P21; white matter, granular layer and molecular layer. (C-C'') P14 white matter analysis include: (C) % of Iba1+ area (P=0.0140, n=4 for both control and mutant), (C') % of Iba1+ cells (P=0.0040, n=4 for both control and mutant) (C") % Iba1+;Edu+ proliferative CNS resident macrophages (P=0.0001, n=4 for both control and mutant). (D-D'') P14 granular layer analysis include: (D) % Iba1+ area (P=0.0155, n=4 for both control and mutant), (D') % Iba1+ cells (P=0.2408, n=4 for both control and mutant) (D") % Iba1+;Edu+ proliferative CNS resident macrophages (P=0.7403, n=4 for both control and mutant). (E-E'') P14 molecular layer analysis include: (E) % Iba1+ area (P=0.2842, n=4 for both control and mutant), (E') % Iba1+ cells (P=0.1506, n=4 for both control and mutant) (E") % Iba1+;Edu+ proliferative CNS resident macrophages (P=0.2153, n=4 for both control and mutant). (F-F'') P21 white matter analysis include: (F) % Iba1+ area (P=0.0023, n=4 for both control and mutant), (F') % Iba1+ cells (P=0.0016, n=4 for both control and mutant) (F") % Iba1+;Edu+ proliferative CNS resident macrophages (P=0.0139, n=4 for both control and mutant). (G-G'') P21 granular layer analysis include: (G) % Iba1+ area (P=0.0309, n=4 for both control and mutant), (D') % Iba1+ cells (P=0.2251, n=4 for both control and mutant) (G") % Iba1+;Edu+ proliferative CNS resident macrophages (P=0.1575, n=4 for both control and mutant). (H-H'') P21 molecular layer analysis include: (H) % Iba1+ area (P=0.1752, n=4 for both control and mutant), (H') % Iba1+ cells (P=0.1344, n=4 for both control and mutant) (H") % Iba1+;Edu+ proliferative CNS resident macrophages (P=0.2093, n=4 for both control and mutant). (I) Altered *Iba1* RNA expression levels (P=0.0317) in mutant cerebellum CNS resident

macrophages normalized to control CNS resident macrophages. (J-J') increased Iba1 protein expression in the whole cerebellum (P=0.0041, n=3 for both control and mutant). Cerebellum regions were labeled with GL for granular layer, ML for molecular layer and WM for white matter.

Supplementary Figure 4

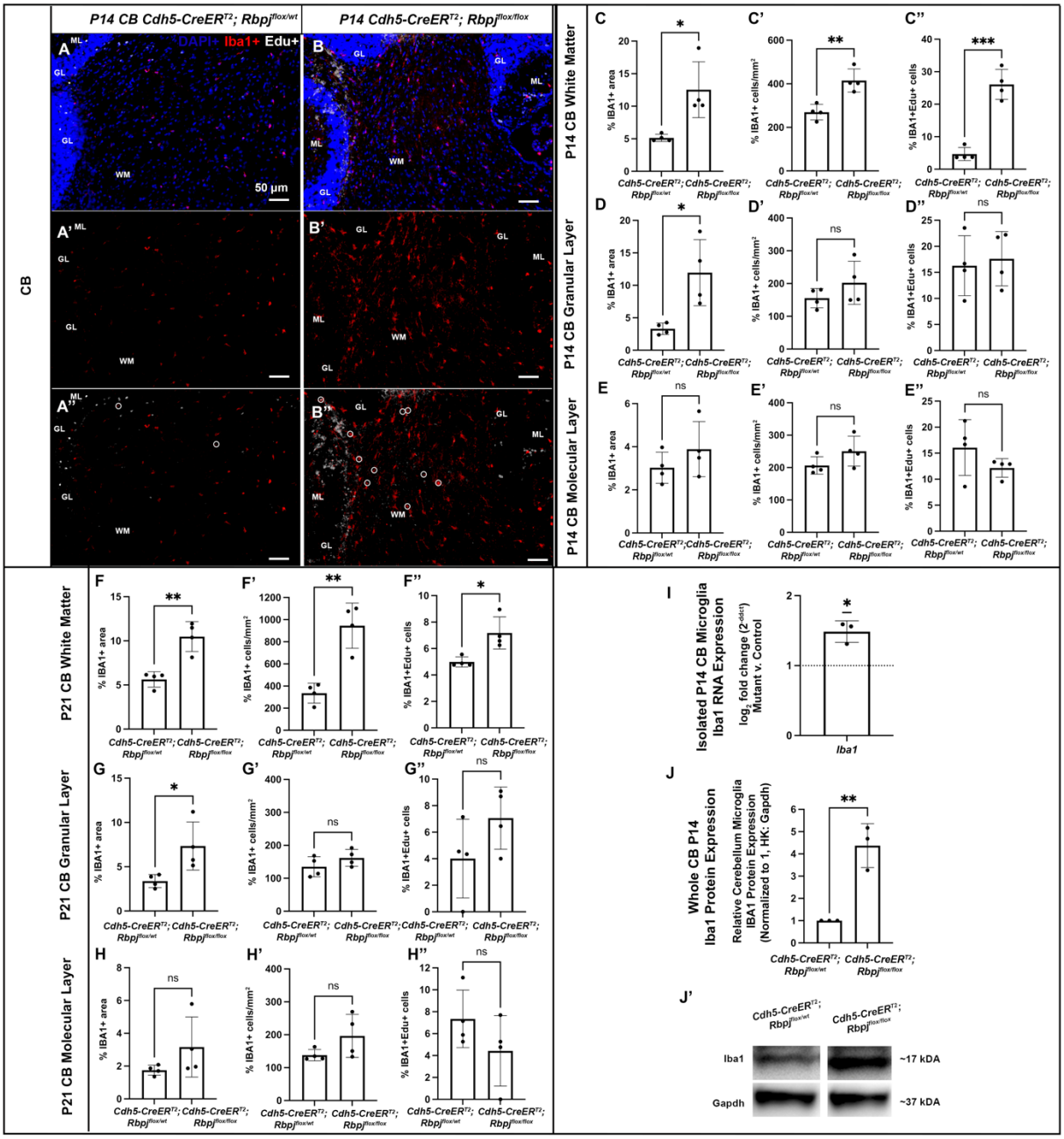

Supplementary Figure 5. No changes in percentage of cell death were found in the cerebellum or the cortex, in control versus mutant brain tissue

Representative images of (A-A'') control P14 and (B-B'') mutant P14 are shown for the cortex. Representative images of (E-E'') control P14 and (F-F'') mutant P14 are shown for the cerebellum. Staining is represented with DAPI in blue for cell nuclei, Iba1+ cells in red, and TUNEL+ apoptotic cells in white. TUNEL+;Iba1+ cells, indicative of apoptotic CNS resident macrophages, are circled in white. The cortex and three cerebellum regions (white matter, granular layer and molecular layer) were analyzed at P14 and P21. Analyses of the cortex include: (C) P14 cortex (P=0.5773, n=3 for both control and mutant) (D) P21 Cortex (P=0.7172, n=3 for both control and mutant). Analyses of the cerebellum include: (G) P14 molecular layer (P=0.3019, n=3 for both control and mutant), (H) P14 granular layer (P=0.2016, n=3 for both control and mutant), (I) P14 white matter (P=0.8992, n=3 for both control and mutant), (J) P21 molecular layer (P=0.5979, n=3 for both control and mutant), (K) P21 granular layer (P=0.4137, n=3 for both control and mutant), (L) P21 white matter (P=0.7084, n=3 for both control and mutant). WM, white matter; GL, granular layer; ML, molecular layer.

Supplementary Figure 5

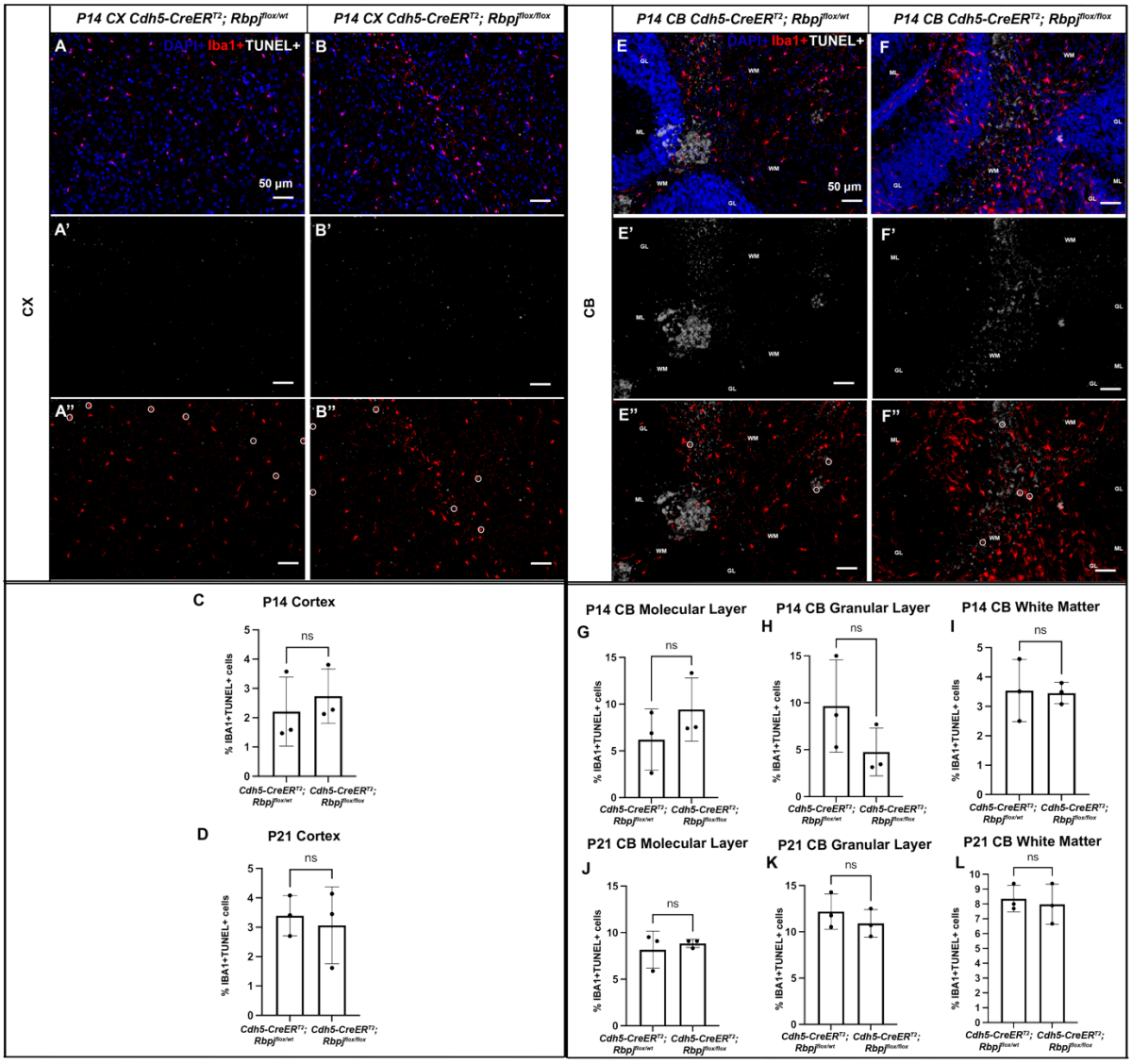

Supplementary Figure 6. Iba1+ cell density was used to distinguish high-Iba1+ density **zone from** low-Iba1+ density **zone, for density scoring**

(A) The high-Iba1+ density zone, marked by '+', is characterized as an area exhibiting at least double the Iba1+ cell density, relative to the low-Iba1+ density zone. (B-D) These panels provide examples of high-Iba1+ density zone scoring, with (B) representing a score of 1, (C) a score of 2, and (D) a score of 3. A score of 0 corresponded to an area where density is similar to that observed in a control sample. (E-F) No change in % TUNEL+;Iba1+ cells in high-Iba1+ density zones versus low-Iba1+ density zones was observed by (E) P14 cortex (P=0.4094, n=3 for both control and mutant) or (F) P21 cortex (P=0.6953, n=3 for both control and mutant).

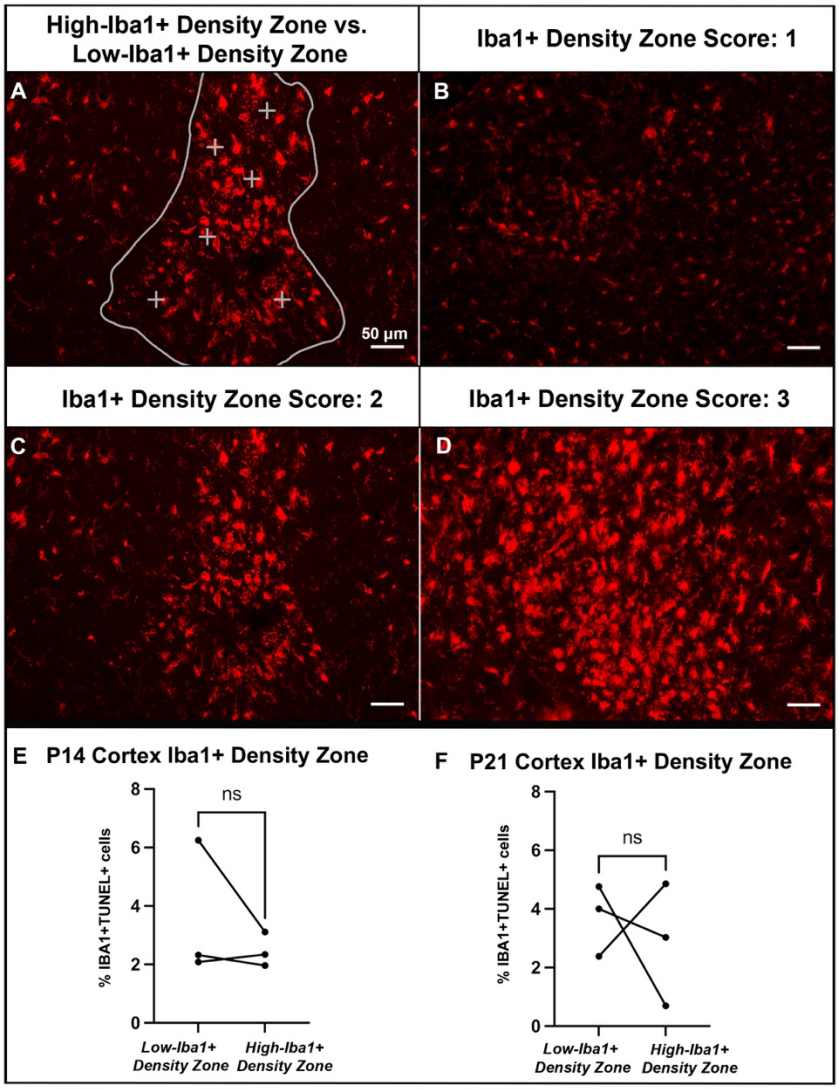

Supplementary Figure 7. CNS resident macrophages cells showed distinct morphological changes in among mutant cerebellum layers, as compared to controls, at P14 and P21

Representative images for (A-B) P14 and (E-F) P21 cerebellum molecular layer; (I-J) P14 and (M-N) P21 cerebellum granular layer; (Q-R) P14 and (U-V) P21 cerebellum white matter. CNS resident macrophages were traced for (A'-B') P14 and (E'-F') P21 molecular layer; (I'-J') P14 and (M'-N') P21 granular layer; (Q'-R') P14 and (U'-V') P21 white matter. Rbpj-mutant white matter showed increased cell body area by (C) P14 (P=0.0098) and (E) P21 (P=0.0095); granular layer showed increased cell body area by (I) P14 (P=0.0009) and (K) P21 (P=0.0010); molecular layer showed no change by (O) P14 (P=0.0623) or (Q) P21(P=0.2326). Rbpj-mutant white matter showed increased process length by (D) P14 (P=0.0003) and (F) P21 (P=0.0249); granular layer showed no change by (J) P14 (P=0.1618) and (L) P21 (P=0.1118); molecular layer showed no change by (P) P14 (P=0.7117) or (R) P21 (P=0.2440) molecular layer. A sample size of n=4 for both control and mutant groups was used.

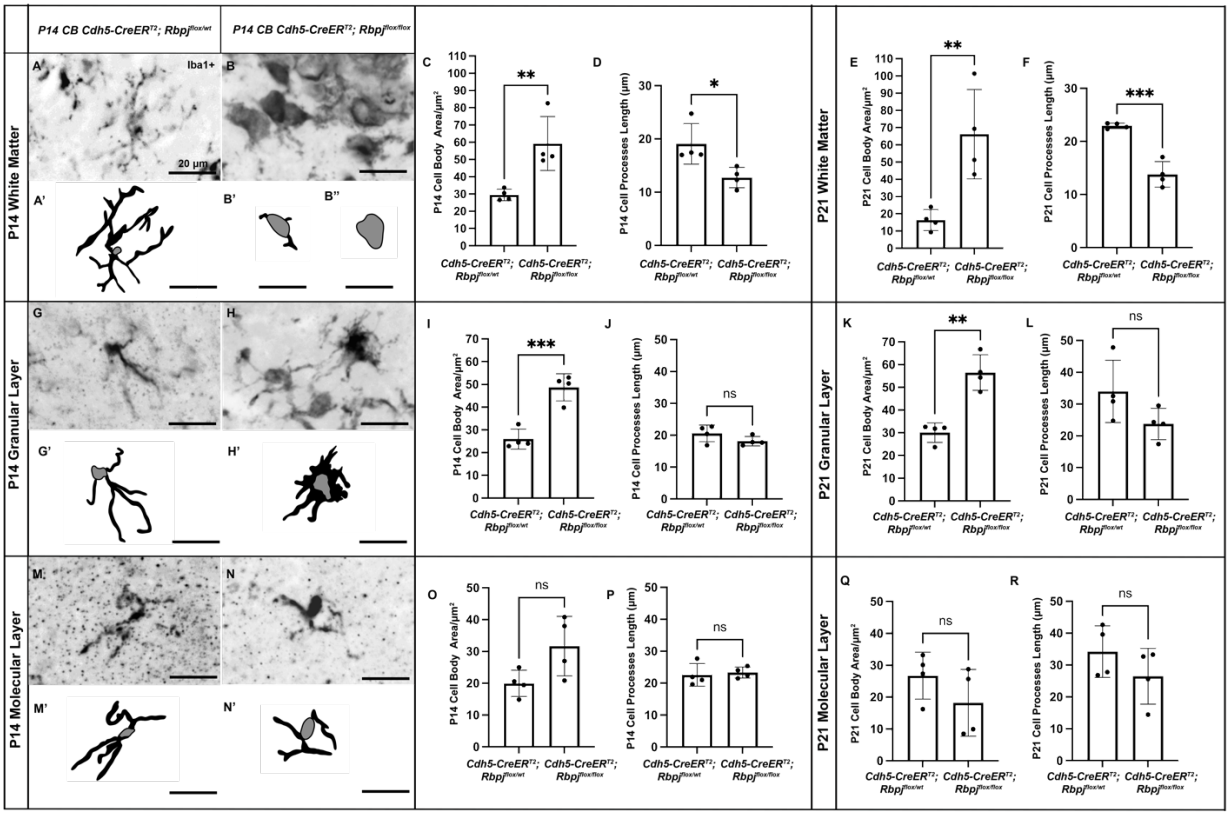

Supplementary Figure 8. Flow cytometry analysis showed shifted CNS resident macrophage states between control and mutant mouse cerebellum at P14

(A-B) Percentages of $CD45^{int/high}$;CD11b+ and $CD45^{low}$;CD11b+ cells isolated from P14 control and mutant whole cerebellum tissue. (C-D) Distribution of $CD45^{int/high}$;CD11b+ cells, as relates to expression of CD206 and CD86. (E) Rbpj-mutant cerebellum showed increased percentage of $CD45^{int/high}$;CD11b+ cells (P=0.0137) and (F) decreased percentage of $CD45^{low}$;CD11b+ cells (P=0.0098), as compared to controls. (G) CNS resident macrophages from mutant and control cerebellum did not fall into distinct subpopulations, based on CD86 and CD206 expression: CD86-;CD206+ (P=0.1271), CD86+;CD206+ (P=0.2116), and CD86+;CD206- (P=N/A). A sample size of n=3 for both control and mutant groups was used, with each analysis encompassing 10,000 events per sample.

Supplementary Figure 8

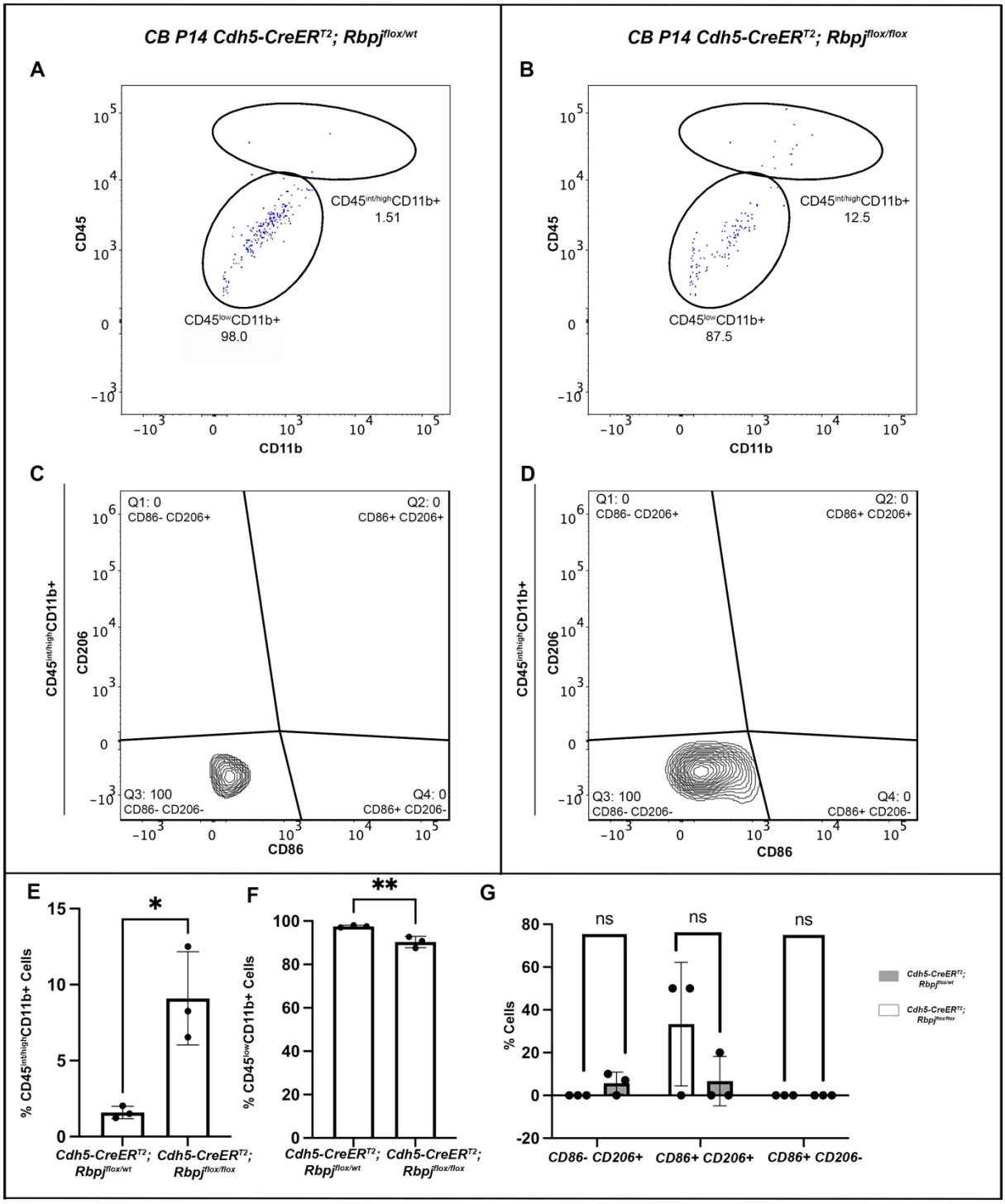

Supplementary Table 1. Primers used for RT-qPCR analysis of transcripts in cortex and cerebellum

Transcript	Forward	Reverse
CD14	TTGAACCTCCGCAACGTGTCGT	CGCAGGAAAAGTTGAGCGAGTG
CD32	AATCCTGCCGTTCCTACTGATC	GTGTCACCGTGTCTTCCTTGAG
IL-10	AGCCGGGAAGACAATAACTG	GGAGTCGGTTAGCAGTATGTTG
Arg1	AATGAAGAGCTGGCTGGTGT	CTGGTTGTCAGGGGAGTGTT
Tgfβ	CCACCTGCAAGACCATCGAC	CTGGCGAGCCTTAGTTTGGAC
CD163	GGCTAGACGAAGTCATCTGCAC	CTTCGTTGGTCAGCCTCAGAGA
Glut5	GGCTCATCTTCCCCTTCATTC	ATGAATGTCCTGCCCTTGG
Glut3	TTCTGGTCGGAATGCTCTTC	AATGTCCTCGAAAGTCCTGC
IBA1	GGACAGACTGCCAGCCTAAG	GACGGCAGATCCTCATCATT
SNAT1	TACCAGAGCACAGGCGACATTC	ATGGCGGCACAGGTGGAACTTT
IL1β	CACCTCTCAAGCAGAGCACAG	GGGTTCCATGGTGAAGTCAAC
TNFα	CCCCAAAGGGATGAGAAGTT	CACTTGGTGGTTTGCTACGA
STAT 1	GCCTCTCATTGTCACCGAAGAAC	TGGCTGACGTTGGAGATCACCA
Clec4e	CCAAGTGCTCTCCTGGACGATA	CTGATGCCTCACTGTAGCAGGA
H2-D1	TGAGGAACCTGCTCGGCTACTA	GGTCTTCGTTCAGGGCGATGTA
H2-Ab1	GTGTGCAGACACAACTACGAGG	CTGTCACTGAGCAGACCAGAGT
Gapdh	AGGGTGGACGTCATTGTAGC	CTGTTGGGGTCTGTCAGGAT

Supplementary Table 2. Cell contamination checks, following adaptation of CNS resident macrophage isolation method for mouse cortex and cerebellum[1]

Effectiveness of brain CNS resident macrophags isolation method was assessed, by determining transcripts from contaminating brain cells. Contamination levels were determined by comparing raw Cq values. *CC10*, a Clara cell (lung)-specific gene, was used as a negative control, while *Gapdh*, a ubiquitously expressed housekeeping gene, was used as a positive control.

Transcript	Cq Value	Cell Type
GFAP	14.874376	Astrocyte
CD13	24.832169	Pericyte
Cdh5	20.365047	Endothelial Cell
Cx3r1	22.715163	Microglia
Mog	26.853581	Oligodendrocyte
Snap5	23.471874	Neuron
CC10	27.402886	Negative Control
Gapdh	13.203978	Positive Control

Supplementary Information References

1. Agalave, N. M., Lane, B. T., Mody, P. H., Szabo-Pardi, T. A. & Burton, M. D. Isolation, culture, and downstream characterization of primary microglia and astrocytes from adult rodent brain and spinal cord. *J. Neurosci. Methods* **340**, 108742 (2020).